Supporting Information

Enhancing Photostability of Perovskite Solar Cells by $Eu(TTA)_2(Phen)MAA$ Interfacial Modification

Wenbo Bi[a], Yanjie Wu[a], Boxue Zhang[a], Junjie Jin[a], Hao Li[a], Le Liu[a], Lin Xu[a], Qilin Dai[b], Cong Chen[a] and Hongwei Song*[a]*

[a] State Key Laboratory on Integrated Optoelectronics, College of Electronic Science and Engineering, Jilin University, 2699 Qianjin Street, Changchun, 130012, People's Republic of China.
E-mail: chencong16@mails.jlu.edu.cn, songhw@jlu.edu.cn
[b] Department of Chemistry, Physics, and Atmospheric Sciences, Jackson State University, Jackson, Mississippi 39217, USA.

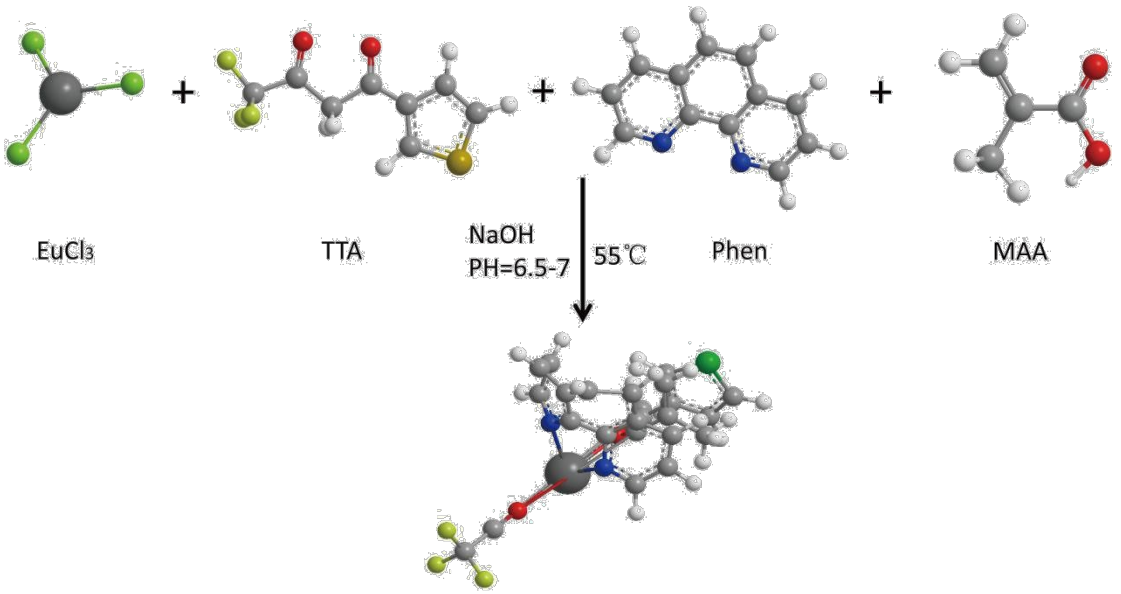

Figure S1. Synthesis route of ETPM (3D model)

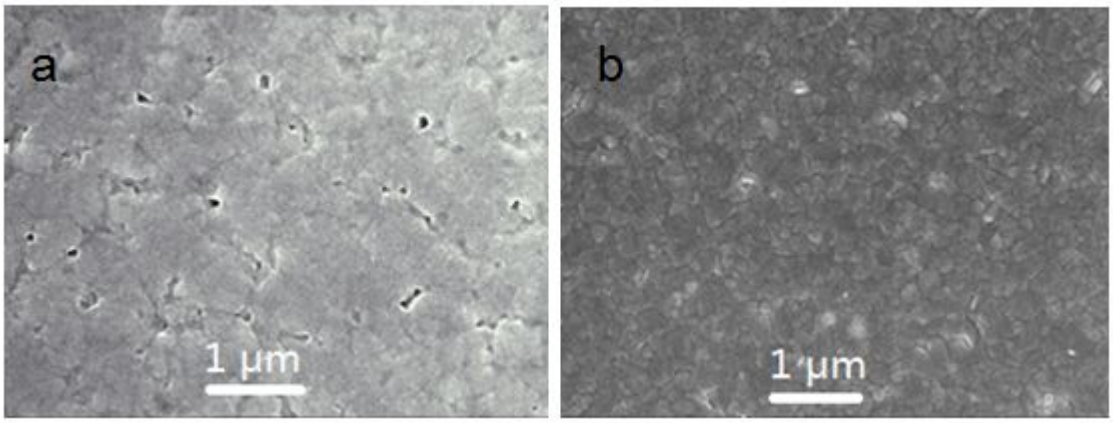

Figure S2. SEM images of perovskite films on (a)control and (b)ETPM modified m-TiO_2 substrate.

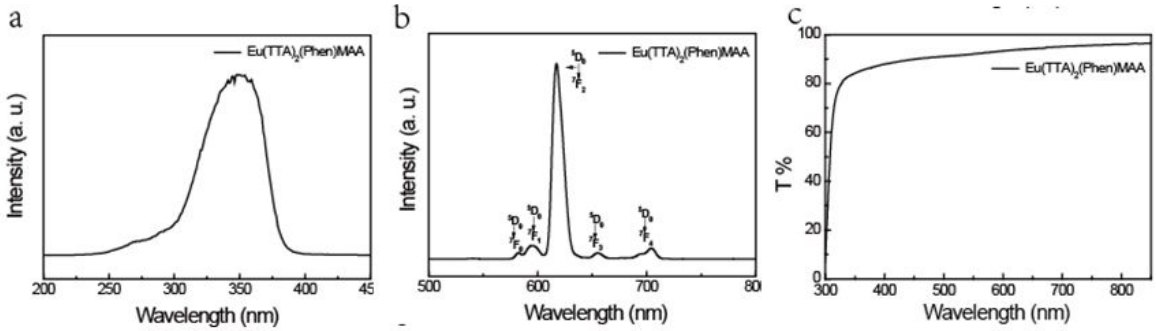

Figure S3. Exciation spectra (a) emission spectra (b) and transmission spectra (c) of ETPM

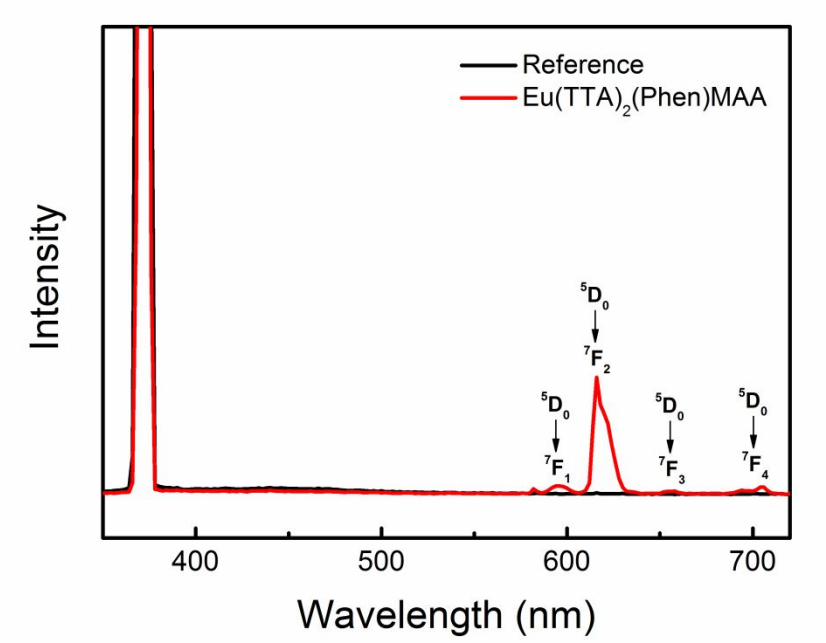

Figure S4. The quantum efficiency of ETPM.

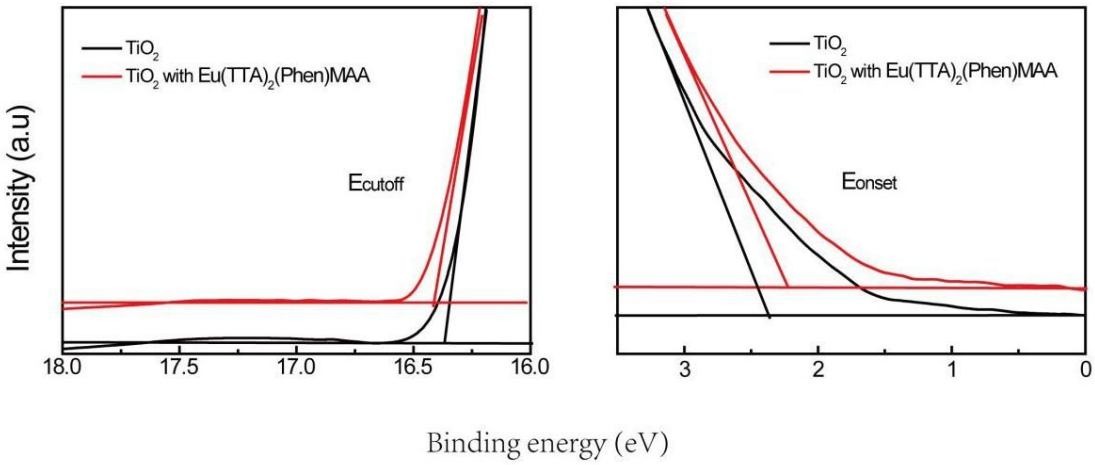

Figure S5. Ultraviolet photoelectron spectra measurements of m-TiO_2 with 1 mg/ml or without ETPM films based on Si substrate

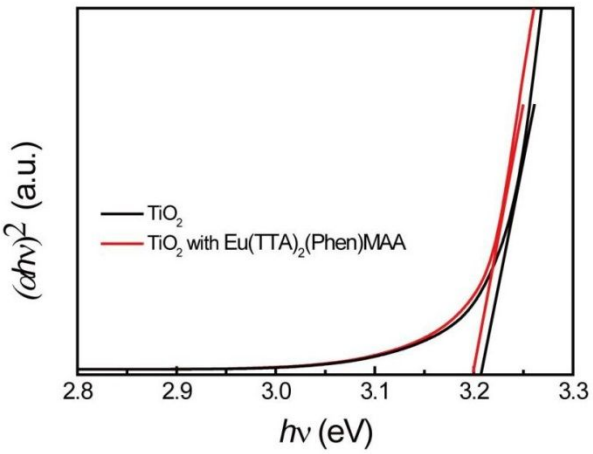

Figure S6. Corresponding plots of $(\alpha h\nu)^2$ and hν for the measurement of the bandgap of m-TiO_2 with 1 mg/ml or without ETPM.

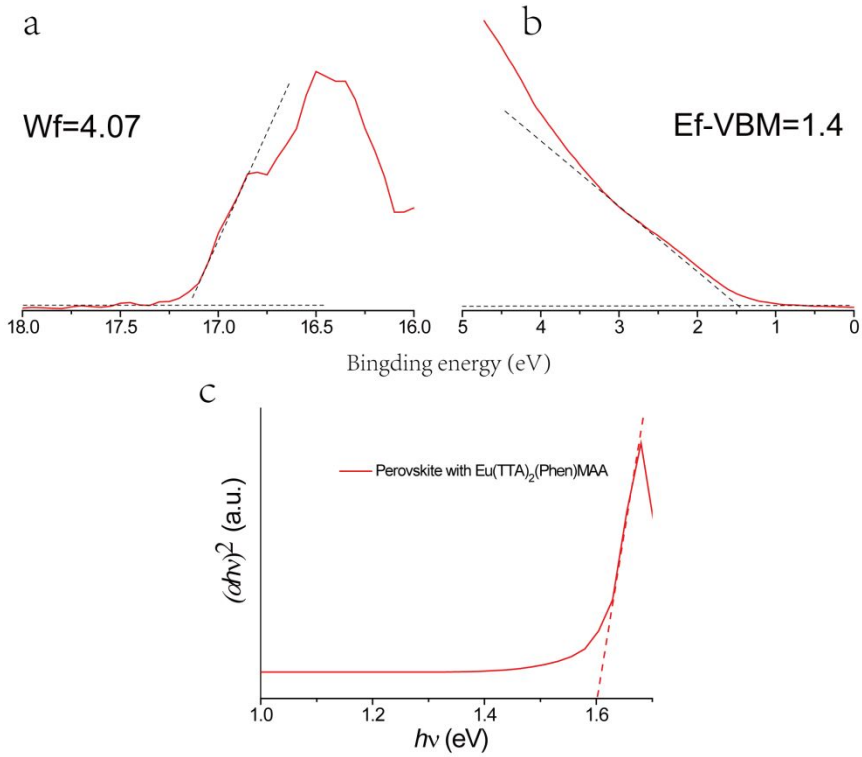

Figure S7. (a) and (b) UPS measurements of perovskite films on Si substrate,(c) corresponding plots of $(\alpha h\nu)^2$ and hν for the measurement of the bandgap of perovskite films.

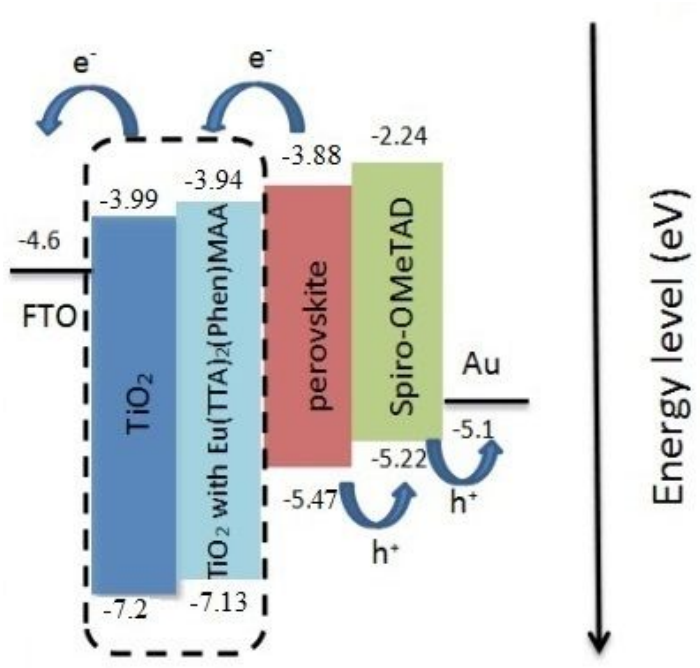

Figure S8. Energy diagram of band alignment for devices based on m-TiO_2 with 1 mg/ml or without ETPM.

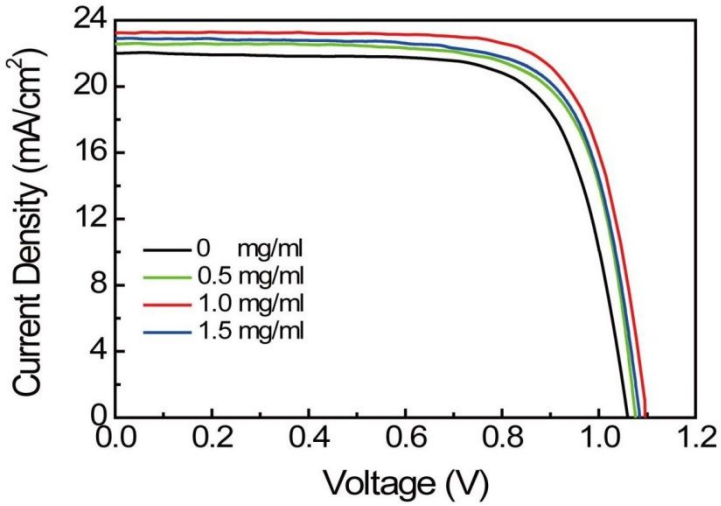

Figure S9. Reverse J–V curves of PSCs with different concentrations of ETPM under simulated AM 1.5G illumination.

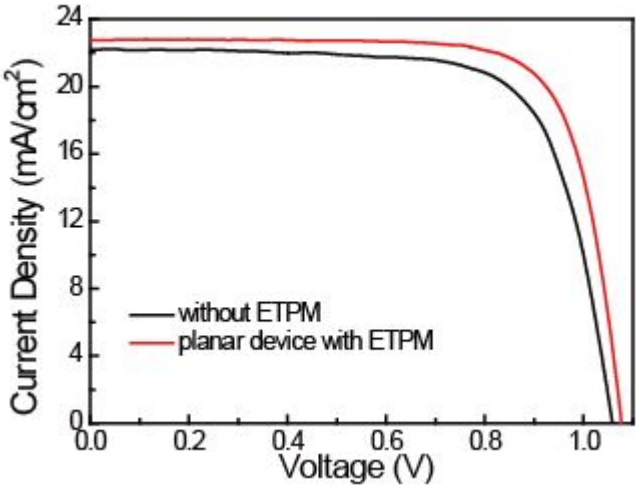

Figure S10. J-V curves of planar devices based on control and ETPM modified c-TiO_2 ETLs.

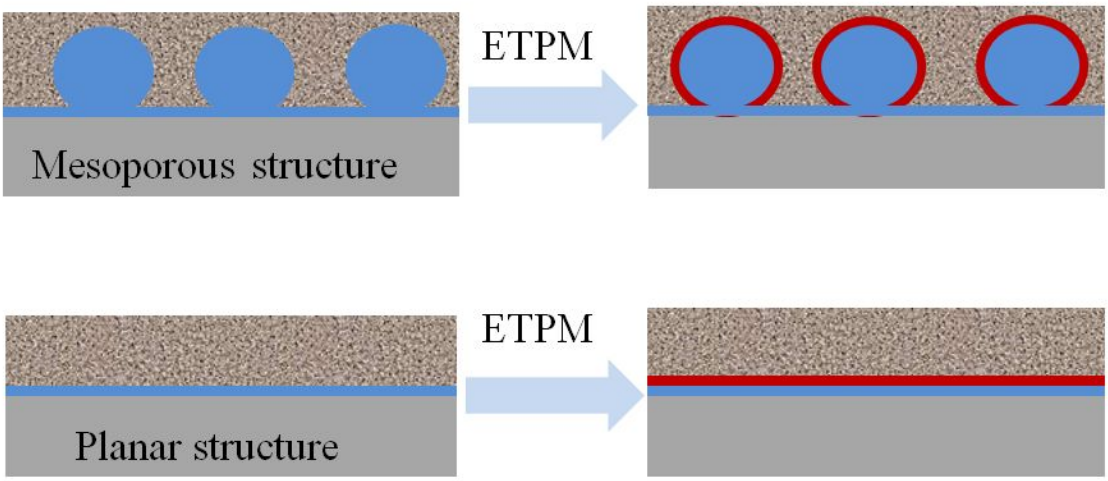

Figure S11. Schematic diagram of ETPM modified on the mesoporous and planar devices.

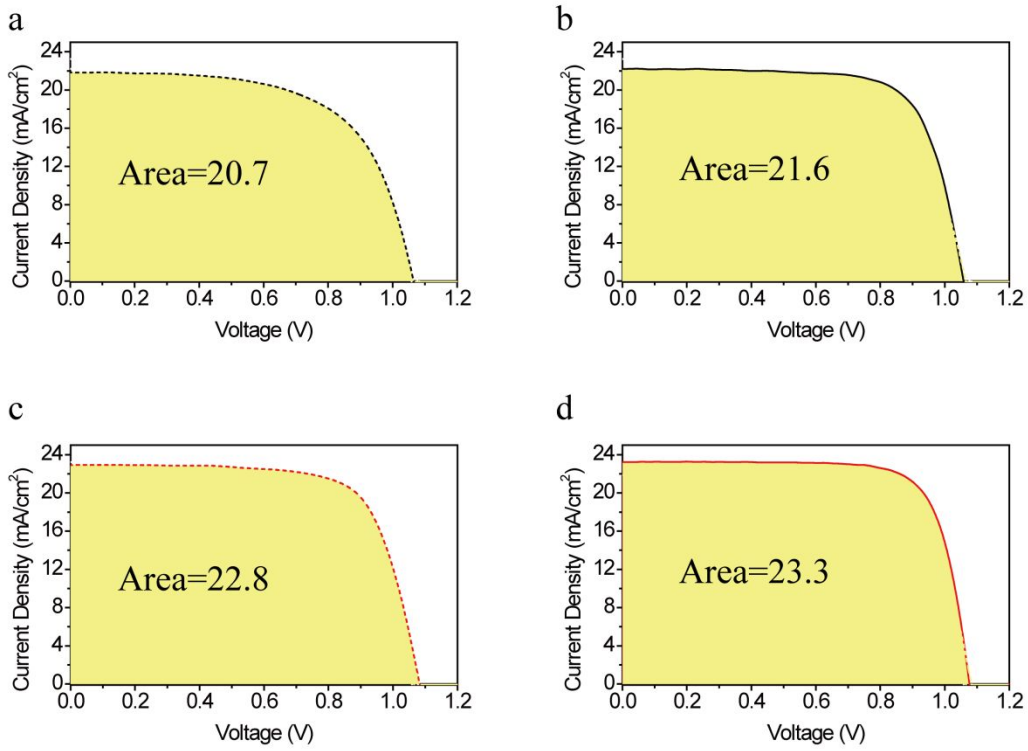

Figure S12. Hysteresis behaviors from J-V curves under different scan directions were measured for devices with or without ETPM. The integral areas are used to calculate HIs. (a) Forward scan and (b) reverse scan for control devices, (c) forward scan and (d) reverse scan for the ETPM modified devices.

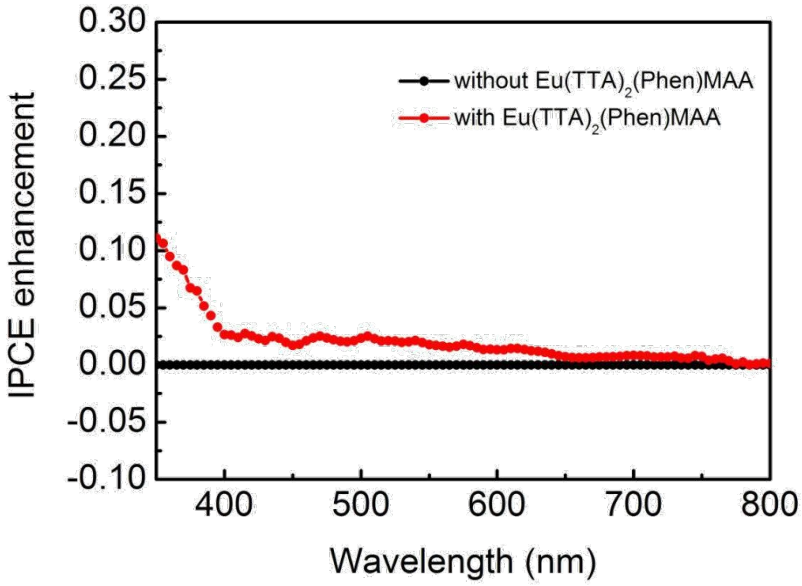

Figure S13. IPCE enhancements of PSCs with optimized concentration or without ETPM.

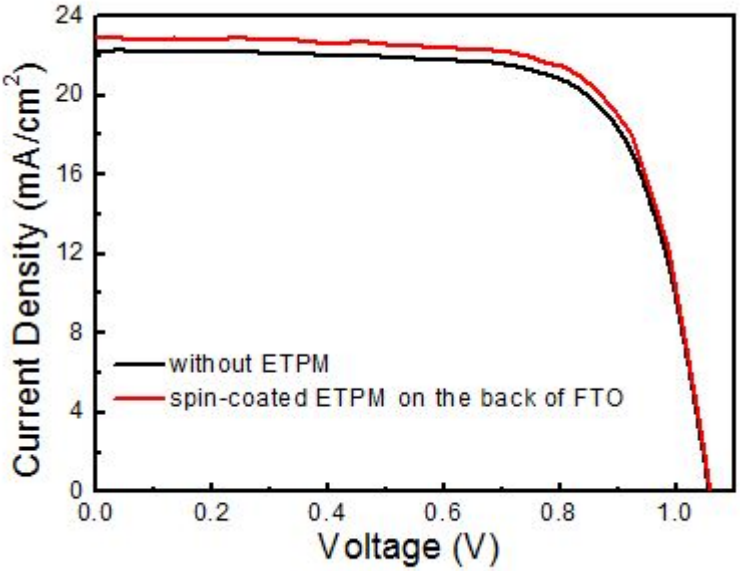

Figure S14. Reverse J–V curves of PSCs without ETPM or spin-coated ETPM on the back of FTO.

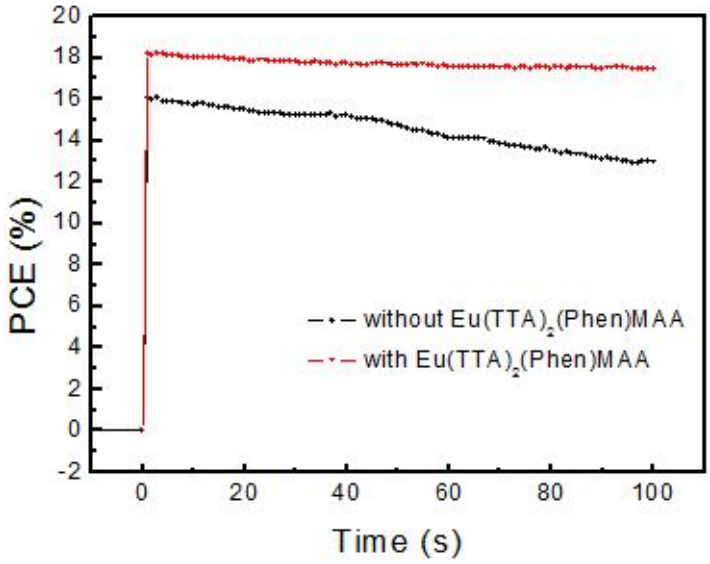

Figure S15. PCE values as a function of time for the control and ETPM modified device under continuous light irradiation.

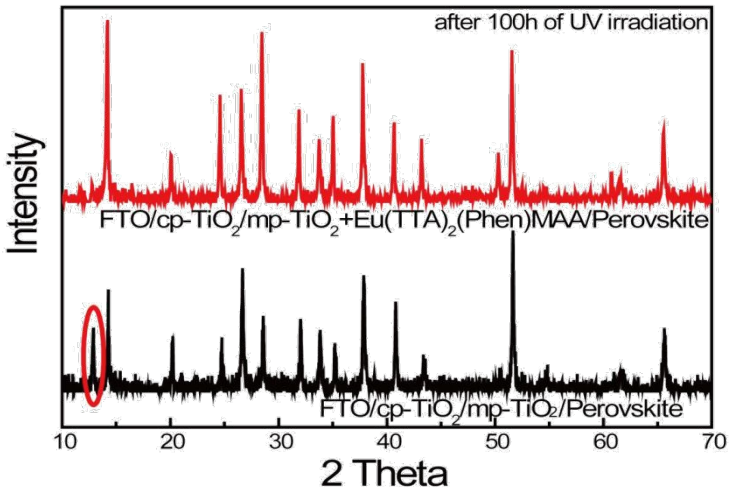

Figure S16 The XRD patterns of perovskite films based on control and ETPM modified TiO_2 substrates under 365nm continuous illumination for 100 h.

Table S1 Atomic content of Eu^{3+} in TiO_2 from XPS.

	Different concentrations of EPTM samples		
	0.5 mg/ml	1.0 mg/ml	1.5 mg/ml
Atomic content of Eu^{3+} (%)	0.84	1.32	1.49

Table S2 Photovoltaic performance of PSCs with different concentrations of ETPM under AM 1.5 illumination.

Concentration of ETPM	Jsc(mA/cm^2)	Voc(V)	FF(%)	PCE(%)
0 mg/ml	22.02	1.06	72.83	17.00
0.5 mg/ml	22.48	1.08	73.73	17.90
1.0 mg/ml	23.23	1.08	76.01	19.07
1.5 mg/ml	22.89	1.08	73.74	18.23